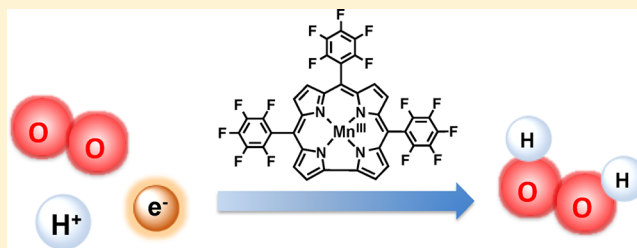


Catalytic Two-Electron Reduction of Dioxygen by Ferrocene Derivatives with Manganese(V) Corroles

Jieun Jung,^{†, ‡} Shuo Liu,[§] Kei Ohkubo,[†] Mahdi M. Abu-Omar,^{*,§} and Shunichi Fukuzumi^{*,†, ‡,||}[†]Department of Material and Life Science, Graduate School of Engineering, Osaka University, ALCA and SENTAN, Japan Science and Technology Agency (JST), Suita, Osaka 565-0871, Japan[‡]Department of Bioinspired Science, Ewha Womans University, Seoul 120-750, Korea[§]Department of Chemistry, Purdue University, 560 Oval Drive, West Lafayette, Indiana 47907, United States^{||}Faculty of Science and Engineering, Meijo University, ALCA and SENTAN, Japan Science and Technology Agency (JST), Nagoya, Aichi 468-0073, Japan

Supporting Information

ABSTRACT: Electron transfer from octamethylferrocene (Me_8Fc) to the manganese(V) imidocorrole complex (tpfc)- $\text{Mn}^{\text{V}}(\text{NAr})$ [tpfc = 5,10,15-tris(pentafluorophenyl)corrole; Ar = 2,6- $\text{Cl}_2\text{C}_6\text{H}_3$] proceeds efficiently to give an octamethylferrocenium ion (Me_8Fc^+) and $[(\text{tpfc})\text{Mn}^{\text{IV}}(\text{NAr})]^-$ in acetonitrile (MeCN) at 298 K. Upon the addition of trifluoroacetic acid (TFA), further reduction of $[(\text{tpfc})\text{Mn}^{\text{IV}}(\text{NAr})]^-$ by Me_8Fc gives (tpfc) Mn^{III} and ArNH_2 in deaerated MeCN. TFA also results in hydrolysis of (tpfc) $\text{Mn}^{\text{V}}(\text{NAr})$ with residual water to produce a protonated manganese(V) oxocorrole complex $[(\text{tpfc})\text{Mn}^{\text{V}}(\text{OH})]^+$ in deaerated MeCN. $[(\text{tpfc})\text{Mn}^{\text{V}}(\text{OH})]^+$ is rapidly reduced by 2 equiv of Me_8Fc in the presence of TFA to give (tpfc) Mn^{III} in deaerated MeCN. In the presence of dioxygen (O_2), (tpfc) Mn^{III} catalyzes the two-electron reduction of O_2 by Me_8Fc with TFA in MeCN to produce H_2O_2 and Me_8Fc^+ . The rate of formation of Me_8Fc^+ in the catalytic reduction of O_2 follows zeroth-order kinetics with respect to the concentrations of Me_8Fc and TFA, whereas the rate increases linearly with increasing concentrations of (tpfc) $\text{Mn}^{\text{V}}(\text{NAr})$ and O_2 . These kinetic dependencies are consistent with the rate-determining step being electron transfer from (tpfc) Mn^{III} to O_2 , followed by further proton-coupled electron transfer from Me_8Fc to produce H_2O_2 and $[(\text{tpfc})\text{Mn}^{\text{IV}}]^+$. Rapid electron transfer from Me_8Fc to $[(\text{tpfc})\text{Mn}^{\text{IV}}]^+$ regenerates (tpfc) Mn^{III} , completing the catalytic cycle. Thus, catalytic two-electron reduction of O_2 by Me_8Fc with (tpfc) $\text{Mn}^{\text{V}}(\text{NAr})$ as a catalyst precursor proceeds via a $\text{Mn}^{\text{III}}/\text{Mn}^{\text{IV}}$ redox cycle.



1. INTRODUCTION

High-valent metal–oxo complexes play an important role in metal-catalyzed oxidation reactions and biological transformations.^{1–11} In particular, manganese(V)–oxo $[\text{Mn}^{\text{V}}(\text{O})]$ is implicated in the four-electron oxidation of water (H_2O) in the oxygen-evolving complex (OEC) of photosystem II. The reactivity of $[\text{Mn}^{\text{V}}(\text{O})]$ complexes has been extensively studied in the context of the four-electron oxidation of H_2O in the OEC of photosystem II.^{12–15} The $\text{Mn}^{\text{V}}(\text{O})$ oxidation state has been stabilized by using trianionic ligands such as corroles, which lack one *meso*-carbon atom in comparison to porphyrins.^{16–20}

The reverse reaction of H_2O oxidation, i.e., the catalytic reduction of dioxygen (O_2) has been studied extensively in relation to the enzymatic function of cytochrome *c* oxidase^{21–23} and also because of its technological significance in fuel cells.^{24,25} The two-electron reduction of O_2 to hydrogen peroxide (H_2O_2) has also attracted increasing interest because H_2O_2 is a versatile and environmentally benign oxidizing reagent produced on a large industrial scale and also because of its potential as a sustainable energy carrier that can be used in

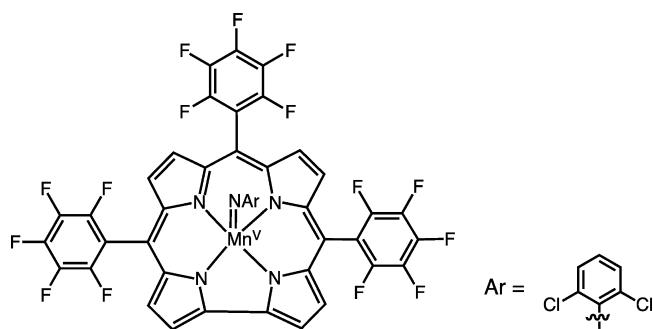
H_2O_2 fuel cells.^{26–29} In comparison to the extensive studies on high-valent manganese(V) complexes in relation to catalytic H_2O oxidation, there has been no report on the role of manganese(V) complexes in O_2 reduction.

We report herein on manganese(V) corrole complexes in the catalytic reduction of O_2 with a one-electron reductant in the presence of acid. We employed the manganese(V) imidocorrole complex $[(\text{tpfc})\text{Mn}^{\text{V}}(\text{NAr})]$ (1), where tpfc = tris(pentafluorophenyl)corrole and Ar = 2,4,6- $\text{Cl}_3\text{C}_6\text{H}_2$ in Scheme 1 as a catalyst precursor for the catalytic reduction of O_2 in the presence of trifluoroacetic acid (TFA) in acetonitrile (MeCN). 1 is known to hydrolyze to produce a manganese(V) oxocorrole complex $[(\text{tpfc})\text{Mn}^{\text{V}}(\text{O})]$.¹⁶ Octamethylferrocene (Me_8Fc) was used as a one-electron chemical reductant for O_2 reduction. Homogeneous systems for O_2 reduction have provided valuable mechanistic insight into the role of reaction intermediates in the catalytic cycle.^{30–36} First, we examined the electron-transfer (ET) reduction of 1 and (tpfc) $\text{Mn}^{\text{V}}(\text{O})$ by

Received: December 16, 2014

Published: April 13, 2015

Scheme 1. Structure of the Manganese(V) Imidocorrole Complex



Me_8Fc in the absence and presence of TFA. In many studies, if the reduced manganese(III) species is oxidized by O_2 to regenerate the $\text{Mn}^{\text{V}}(\text{O})$ species, catalytic four-electron reduction of O_2 by 4 equiv of Me_8Fc would occur. However, we have found that selective two-electron reduction of O_2 by Me_8Fc occurs when **1** is used as a catalyst precursor in the presence of TFA in MeCN. The mechanism of this catalytic two-electron reduction of O_2 is clarified based on detailed kinetic studies of each step in the catalytic cycle as well as the overall catalytic reaction and detection of reactive intermediates.

2. EXPERIMENTAL SECTION

Materials. A manganese(V) imidocorrole complex [(tpfc)- $\text{Mn}^{\text{V}}(\text{NAr})$ (**1**), where tpfc = 5,10,15-tris(pentafluorophenyl)corrole and Ar = 2,6- $\text{Cl}_2\text{C}_6\text{H}_3$] has been synthesized and characterized as reported previously.¹⁶ Octamethylferrocene (Me_8Fc) was obtained commercially and purified by sublimation. Recrystallization of tetra-*n*-butylammonium hexafluorophosphate was performed twice using ethanol and dried *in vacuo* prior to use. Acetonitrile (MeCN) used for spectroscopic and electrochemical measurements was dried with calcium hydride and distilled under dinitrogen (N_2) prior to use.³⁷ All other chemicals were purchased with the best available purity and used without further purification.

Spectroscopic and Kinetic Measurements. Catalytic oxidation of Me_8Fc by O_2 with **1** and TFA in MeCN at 298 K was examined using a Hewlett-Packard 8453 diode-array spectrophotometer. The oxidation rate constants of Me_8Fc to form the corresponding ferrocenium ion (Me_8Fc^+ ; $\lambda_{\text{max}} = 750$ nm and $\epsilon_{\text{max}} = 410$ $\text{M}^{-1}\text{cm}^{-1}$)³⁶ by O_2 were determined from UV-vis spectral changes in the presence of **1** and an excess amount of TFA. The concentration of O_2 in a MeCN solution was controlled by a mixed-gas flow of O_2 and N_2 . The mixed gas was controlled by using a gas mixer (Kofloc GB-3C, Kojima Instrument Inc.), which can mix gases at a certain pressure and flow rate. The concentration of O_2 in an O_2 -saturated MeCN solution (1.3×10^{-2} M) was determined as previously reported.³⁸

After catalytic reduction of O_2 by Me_8Fc with **1** and TFA, the amount of hydrogen peroxide (H_2O_2) formed was determined by adding an excess amount of NaI into the product mixture (20 μL) solution. The amount of I_3^- was determined by the absorption spectrum ($\lambda_{\text{max}} = 361$ nm and $\epsilon_{\text{max}} = 2.8 \times 10^4$ $\text{M}^{-1}\text{cm}^{-1}$).³⁹

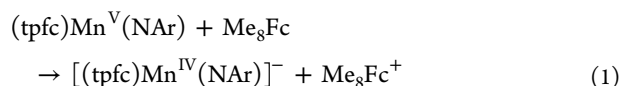
Kinetic measurements for ET with short half-life times (within 10 s) from Me_8Fc to **1** were performed using a UNISOKU RSP-601 stopped-flow spectrophotometer with an MOS-type high selective photodiode array at 298 K. The rates of oxidation of Me_8Fc to give [(tpfc) $\text{Mn}^{\text{IV}}(\text{NAr})$]⁻ (**2**) in MeCN were monitored by an increase of the absorption band due to **2** ($\lambda_{\text{max}} = 468$ nm).

Electron Paramagnetic Resonance (EPR) Measurements. The sample was prepared by adding Me_8Fc (1.0×10^{-3} M) and TFA (2.0×10^{-3} M) into a MeCN solution containing **1** (1.0×10^{-3} M). The solution was stirred and deaerated under an argon atmosphere. After 30 min, the sample was frozen at 4 K. EPR measurements were

performed on a JEOL X-band EPR spectrometer (JES-ME-LX) with a JEOL continuous-flow liquid-helium cryostat coupled to a temperature controller (CT470). The EPR spectra were measured under nonsaturating microwave power conditions. The amplitude of modulation was chosen to optimize the resolution and signal-to-noise (S/N) ratio of the observed spectra. The *g* values were calibrated by using a Mn^{2+} marker.

3. RESULTS AND DISCUSSION

ET from Me_8Fc to **1.** Me_8Fc reduces **1**. The one-electron reduction potential (E_{red}) of **1** was determined to be 0.43 V vs SCE [Figure S1 in the Supporting Information (SI)]. Thus, when Me_8Fc ($E_{\text{ox}} = -0.04$ V vs SCE)^{36a} was employed as an electron donor, ET from Me_8Fc to **1** occurred to produce the corresponding octamethylferrocenium ion (Me_8Fc^+) and **2**, as given in eq 1.



The absorption bands at 376 and 535 nm due to **1** decreased smoothly, accompanied by a rise in the absorption bands at 468 and 622 nm due to **2** (Figure 1a). The stoichiometry of the ET reaction (eq 1) was confirmed by spectral titration at 376 and 468 nm, and no further reduction of **2** occurred, as shown in Figure 1b.

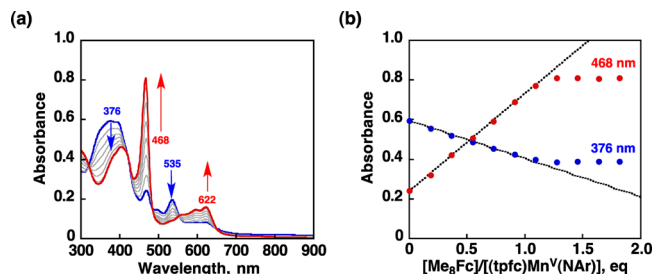


Figure 1. (a) Spectral changes of **1** (1.1×10^{-5} M) upon the addition of Me_8Fc [$(0-2.2) \times 10^{-5}$ M] and (b) absorbance changes at 376 nm (blue) and 468 nm (red) upon the addition of Me_8Fc in deaerated MeCN at 298 K.

The rate of ET from Me_8Fc to **1** in deaerated MeCN was monitored by the appearance of the absorbance peak at 468 nm due to **2** (Figure 2a), following pseudo-first-order kinetics in the presence of excess Me_8Fc (2.0×10^{-4} M) as compared to **1** (1.1×10^{-5} M). The second-order rate constant (k_{red}) was determined to be 9.0×10^3 $\text{M}^{-1}\text{s}^{-1}$ from the slope of the linear

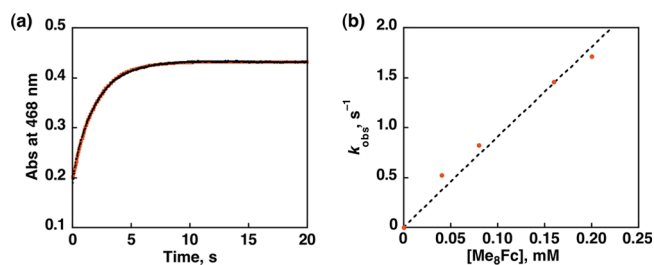


Figure 2. (a) Time profile of the absorption change for the formation of **2** ($\lambda_{\text{max}} = 468$ nm) and the best-fit lines to give a pseudo-first-order rate constant (k_{obs}) in the reduction of **1** (1.1×10^{-5} M) with Me_8Fc (4.0×10^{-5} M) in deaerated MeCN at 298 K. (b) Plots of the observed pseudo-first-order rate constant (k_{obs}) versus concentrations.

plot of the pseudo-first-order rate constant (k_{obs}) versus the concentration of Me_8Fc (Figure 2b). When Me_8Fc was replaced by Me_2Fc ($E_{\text{ox}} = 0.26$ V vs SCE),³⁹ the rate of ET from Me_2Fc to **1** became significantly slower (Figure S2 in the SI).

Reduction of 2 by Me_8Fc in the Presence of TFA. The addition of TFA to the deaerated MeCN solution of **2** and an excess amount of Me_8Fc leads to the conversion of **2** to $(\text{tpfc})\text{Mn}^{\text{III}}$ (**3**),¹⁶ where the absorption bands at 400 and 420 nm due to **3** appeared, accompanied by a decay in the absorption band at 468 nm due to **2**, as shown in Figure 3. The

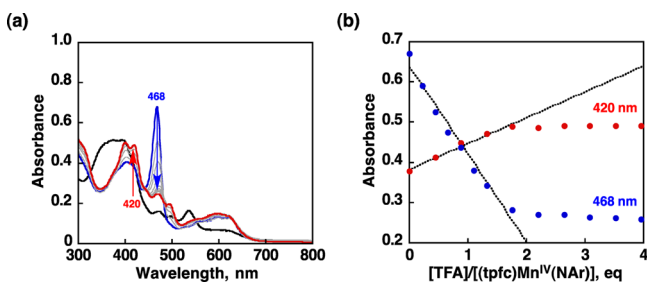
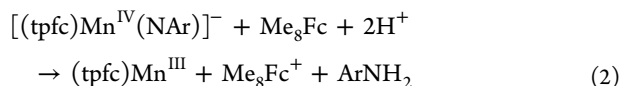


Figure 3. (a) Spectral changes and (b) absorbance changes at 420 and 468 nm starting from **2** produced by the addition of Me_8Fc (1.0×10^{-3} M) to **1** (1.1×10^{-5} M) to generate **3** upon the addition of TFA [$(0-4.4) \times 10^{-5}$ M] in deaerated MeCN at 298 K.

thermodynamics of the hydrogen-atom-transfer process can be analyzed in terms of ET and proton transfer (PT). It was suggested that the proton affinity of **2** allows the manganese(IV) to be reduced to **3**. It has been reported that dissociation of aniline^{16d,e} from high-valent manganese imidocorrole concurrent with the formation of **3** occurred via hydrogen abstraction. Titration of TFA together with **2** can explain the stoichiometry of the PT reaction (eq 2) due to the appearance of **3** at 420 nm and the decay of **2** at 468 nm with 2 equiv of TFA.



Reaction of 1 with TFA. The formation of protonated $\text{Mn}^{\text{V}}(\text{O})$, $[(\text{tpfc})\text{Mn}^{\text{V}}(\text{OH})]^+$ (**4**; $\lambda_{\text{max}} = 420$ nm), was examined by the addition of a strong acid to a MeCN solution of **1** and monitored by UV-vis absorption spectroscopy, as shown in Figure 4a. Upon the addition of TFA to a solution of **1**, spectral changes consistent with **1** transformation to **4** were observed, where 1 equiv of TFA was added to **1** in the presence of residual H_2O in MeCN. The new spectrum assigned to **4**

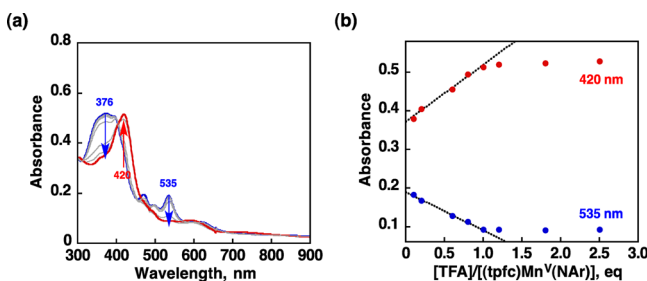
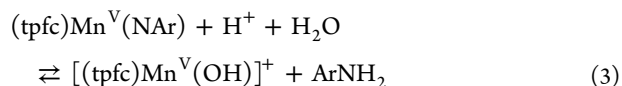


Figure 4. (a) Spectral changes and (b) absorbance changes at 420 and 535 nm starting from **1** (1.1×10^{-5} M) to form **4** upon the addition of TFA [$(0-3.3) \times 10^{-5}$ M] in deaerated MeCN at 298 K.

agrees well with the spectrum obtained from $(\text{tpfc})\text{Mn}^{\text{V}}(\text{O})$ with TFA (Figure S3 in the SI). The equilibrium constant (K_1) for **4** was determined to be 1.0×10^7 M^{-1} according to the protonation equilibrium (eq 3) in Figure 4b, indicating strong association of H^+ to **1**.



No further protonation of **4** was observed in the presence of a large excess TFA (Figure S4 in the SI).

The formation of **4** obeyed pseudo-first-order kinetics over a wide range of TFA concentrations [$(1.0-4.0) \times 10^{-4}$ M] in a deaerated MeCN solution of **1** (1.1×10^{-5} M). Absorbance changes due to **1** at 535 nm upon the addition of TFA versus time were used to obtain a second-order rate constant (k_{H}) of 1.7×10^2 $\text{M}^{-1} \text{s}^{-1}$ from the slope of the linear plot of the pseudo-first-order rate constant (Figure 5b). When the

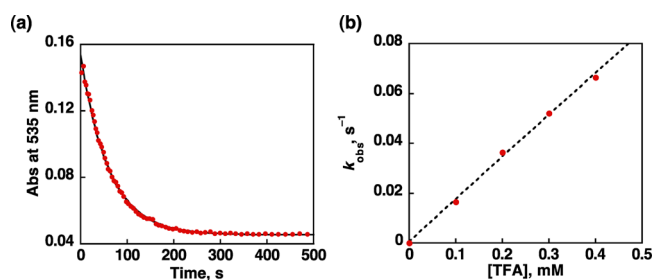
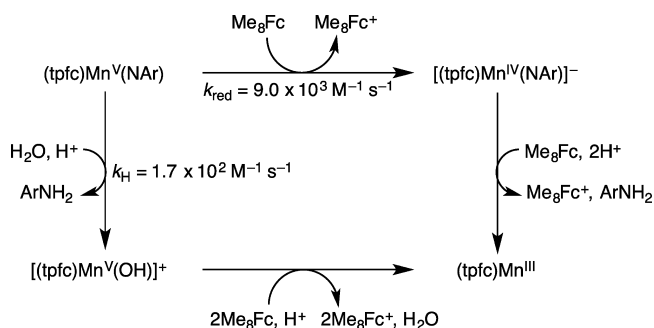


Figure 5. (a) Plots of decay of **1** ($\lambda_{\text{max}} = 535$ nm) versus time and best-fit lines to give the pseudo-first-order rate constant (k_{obs}) of protonation of **1** (1.1×10^{-5} M) with TFA (1.0×10^{-4} M) in deaerated MeCN. (b) Plots of the observed pseudo-first-order rate constant (k_{obs}) versus concentrations of TFA for protonation of **1** (1.1×10^{-5} M) with TFA ($1.0-4.0 \times 10^{-4}$ M) in deaerated MeCN at 298 K.

concentration of H_2O was increased from 1.0×10^{-2} to 2.0×10^{-2} M, the rate of formation of **4** remained constant, indicating that a small amount of H_2O afforded the formation of **4** with TFA.

On the basis of the kinetic study of the reaction of **1** with Me_8Fc and TFA, the mechanisms of PT and ET to **1** are proposed, as shown in Scheme 2. In the presence of Me_8Fc , the conversion from **1** to **2** by ET occurs under pseudo-first-order rate conditions. The addition of TFA to a solution of **2** leads to dissociation of the NAr ligand and rapid conversion to **3**. The reaction of **1** with TFA produces the protonated oxo species **4**, accompanied by dissociation of the imido NAr ligand as ArNH_2

Scheme 2



with residual H₂O in MeCN. **4** generates **3** in the presence of Me₈Fc to form Me₈Fc⁺ and H₂O (Figure S5 in the SI).

Catalytic Two-Electron Reduction of O₂ by Me₈Fc with 1 in the Presence of TFA. The addition of excess Me₈Fc to an O₂-saturated MeCN solution containing a catalytic amount of **1** and TFA resulted in the efficient oxidation of Me₈Fc by O₂ to afford Me₈Fc⁺ (Figure 6). The formation of Me₈Fc⁺ was

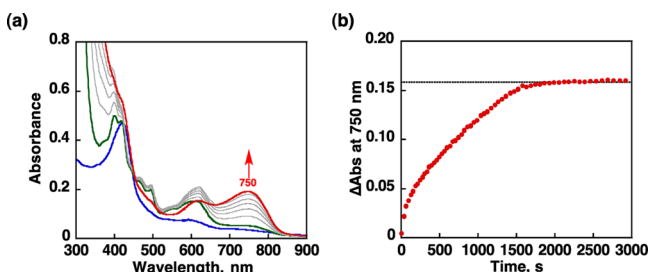
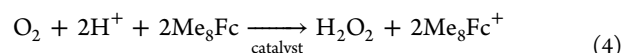


Figure 6. (a) Spectral changes in the two-electron reduction of O₂ (1.3×10^{-2} M) by Me₈Fc (4.0×10^{-4} M) with **1** (1.0×10^{-5} M) in the presence of TFA (1.0×10^{-2} M) in O₂-saturated MeCN at 298 K. The blue and green lines show the spectra before and right after addition of Me₈Fc to a O₂-saturated MeCN of **1** and TFA. (b) Time profile of absorbance at 750 nm due to the formation of Me₈Fc⁺.

monitored by the absorption change at 750 nm, as shown in Figure 6a. Upon the addition of Me₈Fc, **4** (blue line in Figure 6a) produced from **1** in the presence of TFA was converted to

3, as shown by the green-line spectrum, which agrees with the absorption spectrum of **3** (Figure 3a). The catalytic two-electron reduction of O₂ by Me₈Fc was also confirmed to take place with **3** instead of **1** (Figure S6 in the SI). These results suggest that the oxidation of **3** by O₂ is the rate-determining step in the catalytic reaction. Figure 6b shows the time profile for the formation of Me₈Fc⁺ in the reduction of O₂ (1.3×10^{-2} M) catalyzed by **1**. After the catalytic reaction, the formed Me₈Fc⁺ (3.9×10^{-4} M) as the product in the catalytic reduction of O₂ by Me₈Fc is twice the produced amount of H₂O₂ (1.9×10^{-4} M). The formation of a stoichiometric amount of H₂O₂ was confirmed by iodometric titration experiments (Figure S7 in the SI).⁴⁰ Me₈Fc⁺ is quite stable in the presence of TFA in O₂-saturated MeCN, although Me₈Fc⁺ is unstable under basic conditions. The turnover number was determined to be 147. The formation of Me₈Fc⁺ and H₂O₂ did not occur in the absence of O₂ or **1**, indicating that both O₂ and **1** are required to generate H₂O₂ (Figure S8 in the SI). The overall stoichiometry is given by eq 4.



Kinetics and Mechanism of Catalytic Two-Electron Reduction of O₂ by Me₈Fc with 1. The kinetics of catalytic two-electron reduction of O₂ by Me₈Fc with **1** was investigated by following the increase in absorbance at 750 nm due to Me₈Fc⁺ at different concentrations of **1**, Me₈Fc, TFA, and O₂

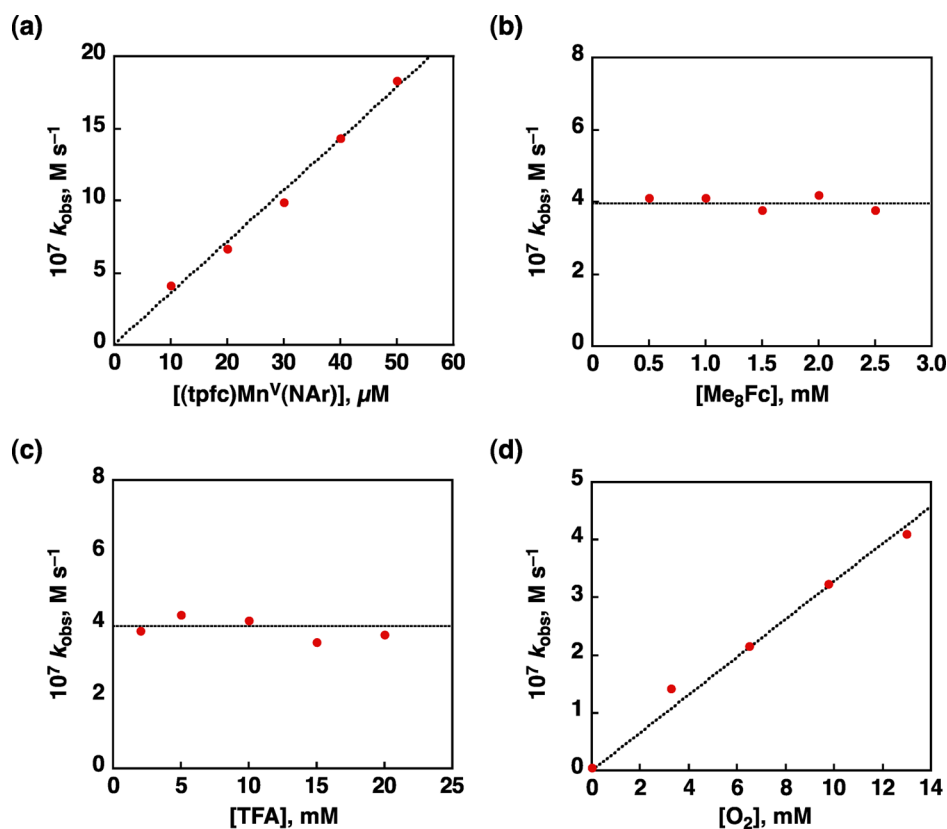
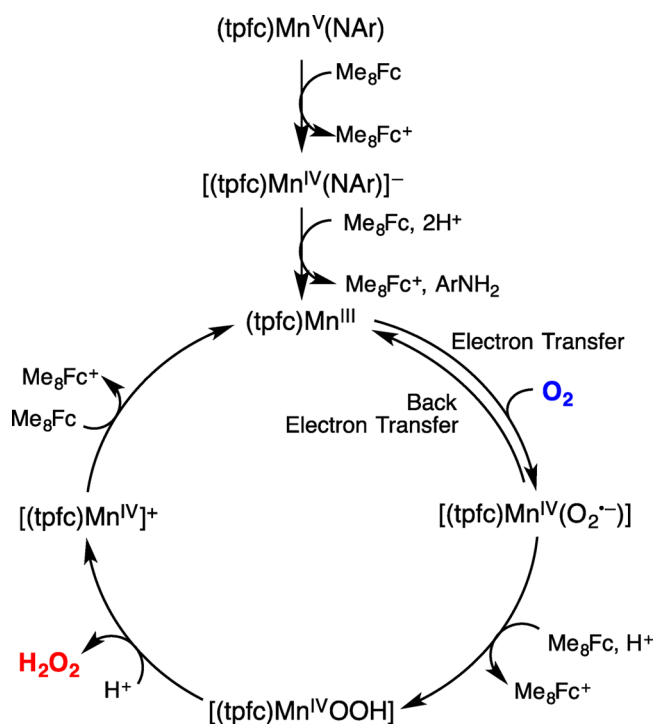


Figure 7. Plot of (a) k_{obs} versus **1** for the two-electron reduction of O₂ (1.3×10^{-2} M) by Me₈Fc (1.0×10^{-3} M) in the presence of TFA (1.0×10^{-2} M) in O₂-saturated MeCN. (b) Plot of k_{obs} versus [Me₈Fc] for the two-electron reduction of O₂ (1.3×10^{-2} M) by various concentrations of Me₈Fc with **1** (1.0×10^{-5} M) in the presence of TFA (1.0×10^{-2} M) in MeCN at 298 K. (c) Plot of k_{obs} versus [TFA] for the two-electron reduction of O₂ (1.3×10^{-2} M) by Me₈Fc (1.0×10^{-3} M) with **1** (1.0×10^{-5} M) in the presence of various concentrations of TFA in MeCN at 298 K. (d) Plot of k_{obs} versus [O₂] for the two-electron reduction of various concentrations of O₂ by Me₈Fc (1.0×10^{-3} M) with **1** (1.0×10^{-5} M) in the presence of TFA (1.0×10^{-2} M) in MeCN at 298 K.

(Figures S9–S12 in the SI). The pseudo-zero-order rate constant (k_{obs}) is proportional to the concentrations of **1** (Figure 7a) and O_2 (Figure 7d), whereas the k_{obs} values remained constant irrespective of the concentrations of Me_8Fc (Figure 7b) and TFA (Figure 7c). The first-order dependence of the rate on the concentrations of **1** and O_2 indicates that inner-sphere ET from **3** to O_2 to give $(\text{tpfc})\text{Mn}^{\text{IV}}(\text{O}_2^{\bullet-})$ is the rate-determining step in the catalytic cycle, as shown in Scheme 3. The produced $(\text{tpfc})\text{Mn}^{\text{IV}}(\text{O}_2^{\bullet-})$ intermediate is reduced

Scheme 3



rapidly by Me_8Fc with H^+ to give $(\text{tpfc})\text{Mn}^{\text{IV}}(\text{OOH})$, which is protonated to release H_2O_2 as a product and $[(\text{tpfc})\text{Mn}^{\text{IV}}]^+$. The latter is reduced rapidly via ET by Me_8Fc , completing the catalytic cycle.

According to Scheme 3, the kinetic equation for the catalytic two-electron reduction of O_2 by Me_8Fc with **1** is given by eq 5, where the k_{cat} value is $2.7 \pm 0.1 \text{ M}^{-1} \text{ s}^{-1}$, calculated from the slopes of the linear plots of k_{obs} versus **1** and $[\text{O}_2]$ in Figure 7.

$$d[\text{Me}_8\text{Fc}^+]/dt = k_{\text{cat}}[(\text{tpfc})\text{Mn}^{\text{V}}(\text{NAr})][\text{O}_2] \quad (5)$$

The mechanism in Scheme 3 is consistent with electrocatalysis of O_2 reduction with metal corroles as previously observed by rotating ring disk electrode voltammetry.⁴¹ Electrocatalysis of O_2 reduction with manganese corrole resulted in two-electron reduction to produce H_2O_2 , whereas iron corroles undergo a four-electron pathway.⁴¹ The ET reduction of O_2 with **3** occurred in the presence of a large excess TFA. When a strong reductant is applied as the electron source, the ET reduction of **3** resulted in the formation of $[(\text{tpfc})\text{Mn}^{\text{II}}]^-$ and $[(\text{tpfc})\text{Mn}^{\text{III}}(\text{O}_2^{\bullet-})]^-$ as O_2 reduction intermediates, which were characterized in the electrochemical O_2 reduction with **3**.

To examine the formation of $[(\text{tpfc})\text{Mn}^{\text{IV}}]^+$ under our steady-state catalysis conditions, EPR measurements were performed, as shown in Figure 8. The EPR spectrum of $[(\text{tpfc})\text{Mn}^{\text{IV}}]^+$ was obtained by the reaction of **3** with 1 equiv of Me_8Fc in the presence of excess amounts of TFA and O_2 . The

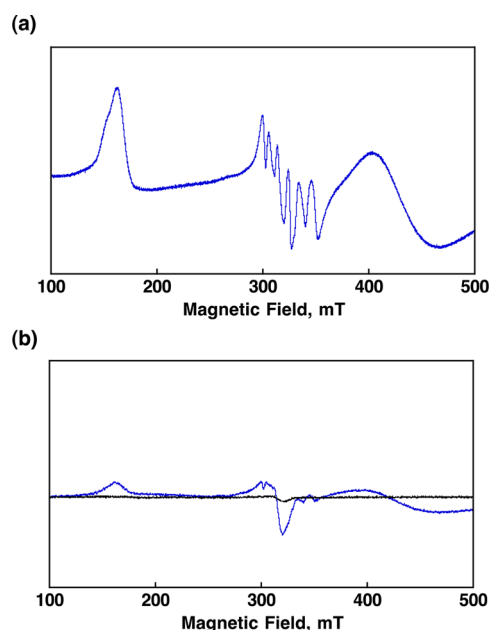


Figure 8. (a) EPR spectrum of $[(\text{tpfc})\text{Mn}^{\text{IV}}]^+$ produced from **3** ($1.0 \times 10^{-3} \text{ M}$) in the presence of Me_8Fc ($1.0 \times 10^{-3} \text{ M}$) and TFA ($1.0 \times 10^{-2} \text{ M}$) in O_2 -saturated MeCN at 4 K. (b) EPR spectrum generated under catalytic conditions from **3** ($1.0 \times 10^{-3} \text{ M}$) in the absence (black) and presence (blue) of Me_8Fc ($8.0 \times 10^{-3} \text{ M}$) and TFA ($1.0 \times 10^{-2} \text{ M}$) in O_2 -saturated MeCN at 4 K, where a reaction solution was immediately frozen after mixing. Experimental parameters: microwave frequency = 9.0 GHz; microwave power = 100 mW; modulation frequency = 1.00 kHz; modulation width = 1.0 mT.

well-resolved spectrum in Figure 8a provides conclusive evidence for the formation of a high-spin manganese(IV) (d^3 , $S = 3/2$) complex. The prominent axial signals of manganese(IV) at $g_{\perp} = 4$ and $g_{\parallel} = 2$ are apparent, being comparable to axial spectra reported previously.^{16d} The EPR spectrum observed under the catalytic conditions with **3** ($1.0 \times 10^{-3} \text{ M}$) and an excess of both Me_8Fc ($8.0 \times 10^{-3} \text{ M}$) and TFA ($1.0 \times 10^{-2} \text{ M}$) in O_2 -saturated MeCN shows a weak signal due to a trace of $[(\text{tpfc})\text{Mn}^{\text{IV}}]^+$, surmising that the reaction of **3** with O_2 is the rate-determining step.

4. CONCLUSIONS

Catalytic two-electron reduction of O_2 by Me_8Fc has been demonstrated with a catalytic amount of **1** in the presence of TFA in MeCN. The rate-determining step in the catalytic cycle is inner-sphere ET from **3** to O_2 to produce a putative superoxide intermediate, $[(\text{tpfc})\text{Mn}^{\text{IV}}(\text{O}_2^{\bullet-})]$, followed by proton-coupled ET reduction to yield H_2O_2 and $[(\text{tpfc})\text{Mn}^{\text{IV}}]^+$; the latter is rapidly reduced by Me_8Fc to regenerate **3**. Thus, catalytic two-electron reduction of O_2 proceeds via a $\text{Mn}^{\text{III}}/\text{Mn}^{\text{IV}}$ redox couple. This is the first report on a homogeneous catalytic two-electron reduction of O_2 to produce H_2O_2 using a manganese complex. This study paves the way to develop manganese-based catalysts for the selective two-electron reduction of O_2 by modifying the ligands to control the redox potentials of the $\text{Mn}^{\text{III}}/\text{Mn}^{\text{IV}}$ couple.

■ ASSOCIATED CONTENT

Supporting Information

Cyclic voltammograms (Figure S1), UV–vis absorption spectral data (Figures S3–S5 and S7), and kinetic analyses

(Figures S2, S6, and S8–S12). This material is available free of charge via the Internet at <http://pubs.acs.org>.

AUTHOR INFORMATION

Corresponding Authors

*E-mail: mabuomar@purdue.edu.

*E-mail: fukuzumi@chem.eng.osaka-u.ac.jp.

Notes

The authors declare no competing financial interest.

ACKNOWLEDGMENTS

This work was supported by an Advanced Low Carbon Technology Research and Development (ALCA) program and a Development of Systems and Technology for Advanced Measurement and Analysis (SENTAN) program from JST to S.F., the Ministry of Education, Culture, Sports, Science and Technology, Japan (Grants-in-Aid 26620154 and 26288037 to K.O.), and the NSF (Grant CHE-1110475 to M.M.A.-O.).

REFERENCES

- (1) (a) *Cytochrome P450: Structure, Mechanism, and Biochemistry*, 3rd ed.; Ortiz de Montellano, P. R., Ed.; Kluwer Academic/Plenum Publishers: New York, 2005. (b) *Metal–Oxo and Metal–Peroxo Species in Catalytic Oxidations*; Meunier, B., Ed.; Springer-Verlag: Berlin, 2000. (c) Terner, J.; Gold, A. J. *Am. Chem. Soc.* **2007**, *129*, 16279–16280. (d) Denisov, I. G.; Makris, T. M.; Sligar, S. G.; Schlichting, I. *Chem. Rev.* **2005**, *105*, 2253–2278.
- (2) (a) Coelho, P. S.; Brustad, E. M.; Kannan, A.; Arnold, F. H. *Science* **2013**, *339*, 307–310. (b) Zhang, R.; Newcomb, M. *Acc. Chem. Res.* **2008**, *41*, 468–477. (c) Meunier, B.; de Visser, S. P.; Shaik, S. *Chem. Rev.* **2004**, *104*, 3947–3980. (d) Franke, A.; Hessenauer-Ilicheva, N.; Meyer, D.; Stochel, G.; Woggon, W.-D.; van Eldik, R. J. *Am. Chem. Soc.* **2006**, *128*, 13611–13624.
- (3) (a) Nam, W. *Acc. Chem. Res.* **2007**, *40*, 522–531. (b) Czernuszewicz, R. S.; Mody, V.; Czader, A.; Gałęzowski, M.; Gryko, D. T. *J. Am. Chem. Soc.* **2009**, *131*, 14214–14215. (c) Shaik, S.; Hirao, H.; Kumar, D. *Acc. Chem. Res.* **2007**, *40*, 532–542. (d) Schmidt, A.-C.; Heinemann, F. W.; Lukens, W. W., Jr.; Meyer, K. J. *Am. Chem. Soc.* **2014**, *136*, 11980–11993.
- (4) (a) Jung, C. *Biochim. Biophys. Acta* **2011**, *1814*, 46–57. (b) Crestoni, M. E.; Fornarini, S. *Inorg. Chem.* **2005**, *44*, 5379–5387. (c) Zhou, M.; Balcells, D.; Parent, A. R.; Crabtree, R. H.; Eisenstein, O. *ACS Catal.* **2012**, *2*, 208–218. (d) Siegbahn, P. E. M. *Acc. Chem. Res.* **2009**, *42*, 1871–1880.
- (5) (a) Tahsini, L.; Bagherzadeh, M.; Nam, W.; de Visser, S. P. *Inorg. Chem.* **2009**, *48*, 6661–6669. (b) Rittle, J.; Green, M. T. *Science* **2010**, *330*, 933–937. (c) Comba, P.; Maurer, M.; Vadivelu, P. *J. Am. Chem. Soc.* **2008**, *112*, 13028–13036.
- (6) (a) Hohenberger, J.; Ray, K.; Meyer, K. *Nat. Commun.* **2012**, *3*, 720–723. (b) Ramdhanie, B.; Telsler, J.; Caneschi, A.; Zakharov, L. N.; Rheingold, A. L.; Goldberg, D. P. *J. Am. Chem. Soc.* **2004**, *126*, 2515–2525. (c) Yoshizawa, K. *Acc. Chem. Res.* **2006**, *39*, 375–382. (d) de Visser, S. P.; Rohde, J.-U.; Lee, Y.-M.; Cho, J.; Nam, W. *Coord. Chem. Rev.* **2013**, *257*, 381–393.
- (7) (a) Buda, B. E. F.; Gribnau, M. C. M.; Baerends, E. J. *J. Am. Chem. Soc.* **2004**, *126*, 4355–4365. (b) Jensen, M. P.; Costas, M.; Ho, R. Y. N.; Kaizer, J.; Payeras, A. M. I.; Münck, E.; Que, L., Jr.; Rohde, J.-U.; Stubna, A. *J. Am. Chem. Soc.* **2005**, *127*, 10512–10525. (c) Shaik, S.; Wang, Y.; Chen, H.; Kumar, D.; Thiel, W. *Chem. Rev.* **2010**, *110*, 949–1017. (d) Harischandra, D. N.; Zhang, R.; Newcomb, M. *J. Am. Chem. Soc.* **2005**, *127*, 13776–13777.
- (8) (a) Tooyama, Y.; Braband, H.; Spingler, B.; Abram, U.; Alberto, R. *Inorg. Chem.* **2008**, *47*, 257–264. (b) Abbina, S.; Bian, S.; Oian, C.; Du, G. *ACS Catal.* **2013**, *3*, 678–684. (c) Abu-Omar, M. M.; Loaiza, A.; Hontzeas, N. *Chem. Rev.* **2005**, *105*, 2227–2252. (d) Gupta, R.; Lacy, D. C.; Bominaar, E. L.; Borovik, A. S.; Hendrich, M. P. *J. Am. Chem. Soc.* **2012**, *134*, 9775–9784.
- (9) (a) Kumar, D.; Hirao, H.; Shaik, S.; Kozłowski, P. M. *J. Am. Chem. Soc.* **2006**, *128*, 16148–16158. (b) Ortiz de Montellano, P. R. *Chem. Rev.* **2010**, *110*, 932–948. (c) Comba, P.; Maurer, M.; Vadivelu, P. *Inorg. Chem.* **2009**, *48*, 10389–10396. (d) Tooyama, Y.; Braband, H.; Spingler, B.; Abram, U.; Alberto, R. *Inorg. Chem.* **2008**, *47*, 257–264.
- (10) (a) Gunay, A.; Theopold, K. H. *Chem. Rev.* **2010**, *110*, 1060–1081. (b) Costas, M. *Coord. Chem. Rev.* **2011**, *255*, 2912–2932. (c) Kumar, D.; Derat, E.; Khenkin, A. M.; Neumann, R.; Shaik, S. *J. Am. Chem. Soc.* **2005**, *127*, 17712–17718. (d) Makris, T. M.; von Koenig, K.; Schlichting, I.; Sligar, S. G. *J. Inorg. Biochem.* **2006**, *100*, 507–518.
- (11) (a) Bart, S. C.; Anthon, C.; Heinemann, F. W.; Bill, E.; Edelstein, N. M.; Meyer, K. *J. Am. Chem. Soc.* **2008**, *130*, 12536–12546. (b) Lacy, D. C.; Gupta, R.; Stone, K. L.; Greaves, J.; Ziller, J. W.; Hendrich, M. P.; Borovik, A. S. *J. Am. Chem. Soc.* **2010**, *132*, 12188–12190. (c) Fernandes, A. C.; Fernandes, J. A.; Romão, C. C.; Veiros, L. F.; Calhorda, M. J. *Organometallics* **2010**, *29*, 5517–5525. (d) Yin, G. *Acc. Chem. Res.* **2013**, *46*, 483–492.
- (12) (a) Umena, Y.; Kawakami, K.; Shen, J.-R.; Kamiya, N. *Nature* **2011**, *473*, 55–60. (b) Slep, L. D.; Mijovilovich, A.; Meyer-Klaucke, W.; Weyhermüller, T.; Bill, E.; Bothe, E.; Neese, E.; Wieghardt, K. *J. Am. Chem. Soc.* **2013**, *125*, 15554–15570. (c) Bigi, J. P.; Harman, W. H.; Lassalle-Kaiser, B.; Robles, D. M.; Stich, T. A.; Yano, J.; Britt, R. D.; Chang, C. J. *J. Am. Chem. Soc.* **2012**, *134*, 1536–1542. (d) Bakac, A. *J. Am. Chem. Soc.* **2000**, *122*, 1092–1097.
- (13) (a) Krebs, C.; Fujimori, D. G.; Walsh, C. T.; Bollinger, J. M. *Acc. Chem. Res.* **2007**, *40*, 484–492. (b) Martinho, M.; Banse, F.; Bartoli, J.-F.; Mattioli, T. A.; Battioni, P.; Horner, O.; Bourcier, S.; Girerd, J.-J. *Inorg. Chem.* **2005**, *44*, 9592–9596. (c) Gunay, A.; Theopold, K. H. *Chem. Rev.* **2010**, *110*, 1060–1081. (d) Yi, C. S.; Zeczycki, T. N.; Guzei, I. A. *Organometallics* **2006**, *25*, 1047–1051.
- (14) (a) Czernuszewicz, R. S.; Mody, V.; Zareba, A. A.; Zaczek, M. B.; Gałęzowski, M.; Sashuk, V.; Grela, K.; Gryko, D. T. *Inorg. Chem.* **2007**, *46*, 5616–5624. (b) Konar, S.; Clearfield, A. *Inorg. Chem.* **2008**, *47*, 3489–3491. (c) King, A. E.; Nippe, M.; Atanasov, M.; Chantarojsiri, T.; Wray, C. A.; Bill, E.; Neese, F.; Long, J. R.; Chang, C. J. *Inorg. Chem.* **2014**, *53*, 11388–11395. (d) Vasbinder, M. J.; Bakac, A. *Inorg. Chem.* **2007**, *46*, 2921–2928.
- (15) (a) Lovell, T.; Han, W.-G.; Liu, T.; Noodleman, L. *J. Am. Chem. Soc.* **2002**, *124*, 5890–5894. (b) Price, J. C.; Barr, E. W.; Tirupati, B.; Bollinger, J. M., Jr.; Krebs, C. *Biochemistry* **2003**, *42*, 7497–7508. (c) Leeladee, P.; Jameson, G. N. L.; Siegler, M. A.; Kumar, D.; de Visser, S. P.; Goldberg, D. P. *Inorg. Chem.* **2013**, *52*, 4668–4682.
- (16) (a) Edwards, N. Y.; Eikey, R. A.; Loring, M. I.; Abu-Omar, M. M. *Inorg. Chem.* **2005**, *44*, 3700–3708. (b) Eikey, R. A.; Abu-Omar, M. M. *Coord. Chem. Rev.* **2003**, *243*, 83–124. (c) Zdilla, M. J.; Abu-Omar, M. M. *J. Am. Chem. Soc.* **2006**, *128*, 16971–16979. (d) Zdilla, M. J.; Dexheimer, J. L.; Abu-Omar, M. M. *J. Am. Chem. Soc.* **2007**, *129*, 11505–11511. (e) Zdilla, M. J.; Abu-Omar, M. M. *Inorg. Chem.* **2008**, *47*, 10718–10722.
- (17) (a) Liu, S.; Mase, K.; Bougher, C.; Hicks, S. D.; Abu-Omar, M. M.; Fukuzumi, S. *Inorg. Chem.* **2014**, *53*, 7780–7788. (b) Zall, C. M.; Clouston, L. J.; Young, V. G., Jr.; Ding, K.; Kim, H. J.; Zhrebetskyy, D.; Chen, Y.-S.; Bill, E.; Gagliardi, L.; Lu, C. C. *Inorg. Chem.* **2013**, *52*, 9216–9228. (c) Groysman, S.; Villagrán, D.; Nocera, D. G. *Inorg. Chem.* **2010**, *49*, 10759–10761.
- (18) (a) Goldberg, D. P. *Acc. Chem. Res.* **2007**, *40*, 626–634. (b) Conradie, J.; Swarts, J. C.; Ghosh, A. *J. Phys. Chem. B* **2004**, *108*, 452–456. (c) Venkataramanan, N. S.; Prem Singh, S.; Rajagopal, S.; Pitchumani, K. *J. Org. Chem.* **2003**, *68*, 7460–7470. (d) Sugimoto, H.; Kitayama, K.; Ashikari, K.; Matsunami, C.; Ueda, N.; Umakoshi, K.; Hosokoshi, Y.; Sasaki, Y.; Itoh, S. *Inorg. Chem.* **2011**, *50*, 9014–9023.
- (19) (a) Meier-Callahan, A. E.; Gray, H. B.; Gross, Z. *Inorg. Chem.* **2000**, *39*, 3605–3607. (b) Vanover, E.; Huang, Y.; Xu, L.; Newcomb, M.; Zhang, R. *Org. Lett.* **2010**, *12*, 2246–2249. (c) Chung, L. W.; Lee, H. G.; Lin, Z.; Wu, Y.-D. *J. Org. Chem.* **2006**, *71*, 6000–6009. (d) Harischandra, D. N.; Lowery, G.; Zhang, R.; Newcomb, M. *Org. Lett.* **2009**, *11*, 2089–2092.

- (20) (a) Gross, Z.; Golubkov, G.; Simkhovich, L. *Angew. Chem., Int. Ed.* **2000**, *39*, 4045–4047. (b) de Visser, S. P.; Ogliaro, F.; Gross, Z.; Shaik, S. *Chem.—Eur. J.* **2001**, *7*, 4954–4960.
- (21) (a) Pereira, M. M.; Santana, M.; Teixeira, M. *Biochim. Biophys. Acta* **2001**, *1505*, 185–208. (b) Winter, M.; Brodd, R. J. *Chem. Rev.* **2004**, *104*, 4245–4270. (c) Ferguson-Miller, S.; Babcock, G. T. *Chem. Rev.* **1996**, *96*, 2889–2907.
- (22) (a) Hosler, J. P.; Ferguson-Miller, S.; Mills, D. A. *Annu. Rev. Biochem.* **2006**, *75*, 165–187. (b) Kaila, V. R. I.; Verkhovskiy, M. I.; Wikström, M. *Chem. Rev.* **2010**, *110*, 7062–7081.
- (23) (a) Von Ballmoos, C.; Lachmann, P.; Gennis, R. B.; Ädelroth, P.; Brzezinski, P. *Biochemistry* **2012**, *51*, 4507–4517. (b) Belevich, I.; Verkhovskiy, M. I. *Antioxid. Redox Signaling* **2008**, *10*, 1–6.
- (24) (a) Vielstich, W.; Lamm, A.; Gasteiger, H. A. *Handbook of fuel cells: fundamentals, technology, and applications*; Wiley: Chichester, U.K., 2003. (b) Zagal, J. H.; Griveau, S.; Silva, J. F.; Nyokong, T.; Bedioui, F. *Coord. Chem. Rev.* **2010**, *254*, 2755–2791. (c) Li, Z. P.; Liu, B. H. *J. Appl. Electrochem.* **2010**, *40*, 475–483. (d) Zagal, J. H.; Gulppi, M.; Isaacs, M.; Cárdenas-Jirón, G.; Aguirre, M. J. *Electrochim. Acta* **1998**, *44*, 1349–1357.
- (25) (a) Li, W.; Yu, A.; Higgins, D. C.; Llanos, B. G.; Chen, Z. *J. Am. Chem. Soc.* **2010**, *132*, 17056–17058. (b) Gewirth, A. A.; Thorum, M. S. *Inorg. Chem.* **2010**, *49*, 3557–3566. (c) Stambouli, A. B.; Traversa, E. *Renewable Sustainable Energy Rev.* **2002**, *6*, 295–304. (d) Marković, N. M.; Schmidt, T. J.; Stamenković, V.; Ross, P. N. *Fuel Cells* **2001**, *1*, 105–116. (e) Steele, B. C. H.; Heinzl, A. *Nature* **2001**, *414*, 345–352. (f) Schechter, A.; Stanevsky, M.; Mahammed, A.; Gross, Z. *Inorg. Chem.* **2012**, *51*, 22–24.
- (26) (a) Yamazaki, S.; Siroma, Z.; Senoh, H.; Ioroi, T.; Fujiwara, N.; Yasuda, K. *J. Power Sources* **2008**, *178*, 20–25. (b) Disselkamp, R. S. *Energy Fuels* **2008**, *22*, 2771–2774. (c) Disselkamp, R. S. *Int. J. Hydrogen Energy* **2010**, *35*, 1049–1053. (d) Fukuzumi, S.; Yamada, Y.; Karlin, K. D. *Electrochim. Acta* **2012**, *82*, 493–511.
- (27) (a) Lei, T.; Tian, Y. M.; Wang, G. L.; Yin, J. L.; Gao, Y. Y.; Wen, Q.; Cao, D. X. *Fuel Cells* **2011**, *11*, 431–435. (b) Hasvold, O.; Storkersen, N. J.; Forseth, S.; Lian, T. J. *Power Sources* **2006**, *162*, 935–942. (c) Patrissi, C. J.; Bessette, R. R.; Kim, Y. K.; Schumacher, C. R. *J. Electrochem. Soc.* **2008**, *155*, B558–B562.
- (28) (a) Yamada, Y.; Yoneda, M.; Fukuzumi, S. *Inorg. Chem.* **2014**, *53*, 1272–1274. (b) Yamada, Y.; Yoneda, M.; Fukuzumi, S. *Chem.—Eur. J.* **2013**, *19*, 11733–11741. (c) Yamada, Y.; Yoshida, S.; Honda, T.; Fukuzumi, S. *Energy Environ. Sci.* **2011**, *4*, 2822–2825. (d) Yamada, Y.; Fukunishi, Y.; Yamazaki, S.; Fukuzumi, S. *Chem. Commun.* **2010**, *46*, 7334–7336.
- (29) (a) Sanli, A. E.; Aytac, A. *Int. J. Hydrogen Energy* **2011**, *36*, 869–875. (b) Jing, X.; Cao, D.; Liu, Y.; Wang, G.; Yin, J.; Wen, Q.; Gao, Y. *J. Electroanal. Chem.* **2011**, *658*, 46–51. (c) Shaegh, S. A. M.; Nguyen, N.-T.; Ehteshami, S. M. M.; Chan, S. H. *Energy Environ. Sci.* **2012**, *5*, 8225–8228.
- (30) (a) Fukuzumi, S. *Chem. Lett.* **2008**, *37*, 808–813. (b) Fukuzumi, S.; Tahsini, L.; Lee, Y.-M.; Ohkubo, K.; Nam, W.; Karlin, K. D. *J. Am. Chem. Soc.* **2012**, *134*, 7025–7035. (c) Fukuzumi, S.; Mandal, S.; Mase, K.; Ohkubo, K.; Park, H.; Benet-Buchholz, J.; Nam, W.; Llobet, A. *J. Am. Chem. Soc.* **2012**, *134*, 9906–9909. (d) Wada, T.; Maki, H.; Imamoto, T.; Yuki, H.; Miyazato, Y. *Chem. Commun.* **2013**, *49*, 4394–4396.
- (31) (a) McGuire, R., Jr.; Dogutan, D. K.; Teets, T. S.; Suntivich, J.; Shao-Horn, Y.; Nocera, D. G. *Chem. Sci.* **2010**, *1*, 411–414. (b) Dogutan, D. K.; Stoian, S. A.; McGuire, R., Jr.; Schwalbe, M.; Teets, T. S.; Nocera, D. G. *J. Am. Chem. Soc.* **2011**, *133*, 131–140. (c) Teets, T. S.; Cook, T. R.; McCarthy, B. D.; Nocera, D. G. *J. Am. Chem. Soc.* **2011**, *133*, 8114–8117. (d) Decréau, R. A.; Collman, J. P.; Hosseini, A. *Chem. Soc. Rev.* **2010**, *39*, 1291–1301.
- (32) (a) Olaya, A. J.; Schaming, D.; Brevet, P.-F.; Nagatani, H.; Zimmermann, T.; Vanicek, J.; Xu, H.-J.; Gros, C. P.; Barbe, J.-M.; Girault, H. H. *J. Am. Chem. Soc.* **2011**, *134*, 498–506. (b) Peljo, P.; Murtoimäki, L.; Kallio, T.; Xu, H.-J.; Meyer, M.; Gros, C. P.; Barbe, J.-M.; Girault, H. H.; Laasonen, K.; Kontturi, K. *J. Am. Chem. Soc.* **2012**, *134*, 5974–5984. (c) Su, B.; Hatay, I.; Trojanek, A.; Samec, Z.; Khoury, T.; Gros, C. P.; Barbe, J.-M.; Daina, A.; Carrupt, P.-A.; Girault, H. H. *J. Am. Chem. Soc.* **2010**, *132*, 2655–2662. (d) Schechter, A.; Stanevsky, M.; Mahammed, A.; Gross, Z. *Inorg. Chem.* **2012**, *51*, 22–24.
- (33) (a) Halime, Z.; Kotani, H.; Li, Y.; Fukuzumi, S.; Karlin, K. D. *Proc. Natl. Acad. Sci. U.S.A.* **2011**, *108*, 13990–13994. (b) Schwalbe, M.; Dogutan, D. K.; Stoian, S. A.; Teets, T. S.; Nocera, D. G. *Inorg. Chem.* **2011**, *50*, 1368–1377. (c) Masa, J.; Ozoemena, K.; Schuhmann, W.; Zagal, J. H. *J. Porphyrins Phthalocyanines* **2012**, *16*, 761–784. (d) Chen, P.; Lau, H.; Habermeyer, B.; Gros, C. P.; Barbe, J. M.; Kadish, K. M. *J. Porphyrins Phthalocyanines* **2011**, *15*, 467–479.
- (34) (a) Carver, C. T.; Matson, B. D.; Mayer, J. M. *J. Am. Chem. Soc.* **2012**, *134*, 5444–5447. (b) Matson, B. D.; Carver, C. T.; Von Ruden, A.; Yang, J. Y.; Raugei, S.; Mayer, J. M. *Chem. Commun.* **2012**, *48*, 11100–11102. (c) Warren, J. J.; Tronic, T. A.; Mayer, J. M. *Chem. Rev.* **2010**, *110*, 6961–7001.
- (35) (a) Kakuda, S.; Peterson, R. L.; Ohkubo, K.; Karlin, K. D.; Fukuzumi, S. *J. Am. Chem. Soc.* **2013**, *135*, 6513–6522. (b) Das, D.; Lee, Y.-M.; Ohkubo, K.; Nam, W.; Karlin, K. D.; Fukuzumi, S. *J. Am. Chem. Soc.* **2013**, *135*, 2825–2834. (c) Fukuzumi, S.; Karlin, K. D. *Coord. Chem. Rev.* **2013**, *257*, 187–195. (d) Kakuda, S.; Rolle, C. J.; Ohkubo, K.; Siegler, M. A.; Karlin, K. D.; Fukuzumi, S. *J. Am. Chem. Soc.* **2015**, *137*, 3330–3337.
- (36) (a) Tahsini, L.; Kotani, H.; Lee, Y.-M.; Cho, J.; Nam, W.; Karlin, K. D.; Fukuzumi, S. *Chem.—Eur. J.* **2012**, *18*, 1084–1093. (b) Fukuzumi, S.; Kotani, H.; Lucas, H. R.; Doi, K.; Suenobu, T.; Peterson, R. L.; Karlin, K. D. *J. Am. Chem. Soc.* **2010**, *132*, 6874–6875. (c) Mase, K.; Ohkubo, K.; Fukuzumi, S. *J. Am. Chem. Soc.* **2013**, *135*, 2800–2808. (d) Mase, K.; Ohkubo, K.; Fukuzumi, S. *Inorg. Chem.* **2015**, *54*, 1808–1815. (e) Honda, T.; Kojima, T.; Fukuzumi, S. *J. Am. Chem. Soc.* **2012**, *134*, 4196–4206.
- (37) Armarego, W. L. F.; Chai, C. L. L. *Purification of Laboratory Chemicals*, 7th ed; Pergamon Press: Oxford, U.K., 2013.
- (38) (a) Fukuzumi, S.; Ishikawa, M.; Tanaka, T. *J. Chem. Soc., Perkin Trans. 2* **1989**, 1037–1045. (b) Fukuzumi, S.; Ohkubo, K. *Chem.—Eur. J.* **2000**, *6*, 4532–4535.
- (39) Das, D.; Lee, Y.-M.; Ohkubo, K.; Nam, W.; Karlin, K. D.; Fukuzumi, S. *J. Am. Chem. Soc.* **2013**, *135*, 4018–4026.
- (40) Fukuzumi, S.; Kuroda, S.; Tanaka, T. *J. Am. Chem. Soc.* **1985**, *107*, 3020–3027.
- (41) (a) Collman, J. P.; Kaplun, M.; Decréau, R. A. *Dalton Trans.* **2006**, 554–559. (b) Bard, A. J.; Faulkner, L. R. *Electrochemical Methods*; Wiley: New York, 2001.